Precise finite element verification of the unreliability of using multi-layers of FRP on CFRP-debonding in RC beams

Bassam Qasim Abdulrahman

Abstract

The nonlinear behaviour of an adhesive material that connects layer of carbon fibre reinforced polymer (CFRP) to a reinforced concrete (RC) beam is numerically simulated in this study. To the author's knowledge, how debonding increases significantly with increasing FRP thickness has not yet been studied theoretically only with few experimental studies that directly say this information. The work is conducted via a finite element approach using the commercially available software ABAQUS 6.13. Firstly, the 3D finite element model is introduced and all the suitable elements, material properties, damage initiation and evolution, and failure criteria are presented. Initially, the numerical model is validated by using the experimental study of a CFRP strengthened beam, which is chosen from literature. The model is shown to accurately capture slip at the interface of the strengthening material and resultant debonding. Furthermore, the tensile strain profile along the CFRP sheet is studied and, which has shown a reverse trend to the interfacial slip profile. Using the validated model, a detailed study is conducted with regards to the effects of multiple CFRP layers on the ultimate capacity and failure mode of the strengthened RC beam. It is found that adding two layers similar to the thickness of one layer will not change the response of the beam. However, this makes the beam behave with less ductility. Furthermore, the difference between the two cases is that the damage of one layer is concentrated at the FRP free end for a short distance. While, for two layers it is also at the free end but extended to a longer distance to the centre of the beam what causes earlier debonding. It is also found that adding one layer of CFRP to strengthen a RC beam can improve the ultimate capacity by 22%. But adding more CFRP layers does not increase the ultimate capacity or change the failure mode. In addition, it will reduce the total deflection of the beam. The study has also found that the interface bond-stresses are non-uniformly distributed along the reinforced boundaries and the shear stresses values exhibit peak values of 1

to 2 times greater than or 1 to 0.5 times less than the mean values predicted by the classical beam theory. Moreover, during the simulation, no de-lamination was observed between the superimposed CFRP plates for the two layers of CFRP.

Key-word: CFRP, Strengthening, Reinforced concrete beams, Debonding, Cohesive model, Finite element analysis (FEA), Multi layers, Bond-slip models

1- Introduction

Over the last few decades FRP composites have been used in civil engineering, especially in the structural strengthening and repairing due to their relatively high stiffness, strength to weight ratio and the high resistance to the environmental effects [1, 2]. It is well understood that bonding FRP composites to the concrete soffit can improve the structural performance of reinforced concrete members. The most important aspect of the strengthening RC structures by FRP is the transmission of shear and normal stresses at the plate-concrete interface especially in material discontinuities [3, 4]. And thus, the FRP-concrete bond is the main factor that affects both the efficiency and the mechanical behaviour of the strengthened sections [5, 6]. Therefore, the mechanical properties and the failure mechanism are totally related to the bond characteristics of the FRP-concrete interface.

There are still concerns regarding the effectiveness and safety of this strengthening method due to the brittle debonding failure. Recently, many studies have been conducted experimentally and theoretically on the static behaviour of RC beams that externally strengthened with FRP composites. The simplest case was derived based on the pure shear analysis, in which the interfacial stresses are totally related to the slippage between the FRP composite and the concrete substrate as it was described by [7, 8, 9, and 10]. In all these studies, it was assumed that the materials exhibit linear elastic behaviour and the stress is constant across the adhesive.

One of the most important factors that affect bond is the mechanical property of the adhesive. Debonding failure can be prompted by improper selection of adhesives. Nowadays, manufacturers are producing adhesives with tensile strength and bond strength higher than the concrete tensile strength. Reinforced concrete beams are usually strengthened by one layer of CFRP sheets in order to increase their capacity.

Pre-formed FRP plates or sheets are manufactured in standard thickness; as a result, multiple layers of CFRP may be needed to achieve the total thickness of strengthening required in some cases. In such circumstances, the interlayer behaviour of the CFRP and subsequent performance may be different to that of a monolithic plate of the same total thickness.

In more detailed analysis in which the variation in stress across the adhesive is considered, a more complex solutions were naturally leaded. Early studies by Oehlers and Moran [11] had stated that the main cause of debonding failure was the shear stresses of the interface. They had also given an empirical method to calculate the debonding failure. Later studies had shown that the debonding failure was related to the interface normal stresses not only to the interface shear stresses [12-15]. Li et al [16] found that the FRP thickness has a major influence on the crack pattern and the failure mode. Furthermore, they found that the bi-layer strengthening of RC beams can efficiently restrain the crack development. In their research, they have not explained the mechanism in which bi-layer strengthening influences the failure mode and ultimate load capacity. Harajli and Soudki [17] used two CFRP layers in strengthening RC slabs against punching shear. They noticed that using two CFRP layers results in larger force in the sheets and consequently larger concentration of horizontal shear at the interface between CFRP sheets and the concrete. Garden et al [18] tested reinforced concrete beams strengthened by CFRP composites. One of these beams was strengthened by additional CFRP sheet to anchor the plate end against delamination. In their study, they found that the interface between the adhesive and the plate was damaged near the failed end of the plate. They also explained that failure was due to the propagation of the concrete shear cracks through the adhesive along the plate-adhesive interface. They also found that debonding increases significantly with increasing FRP thickness for a fixed FRP ratio. However, anchoring the plate end by additional FRP plate prevented the FRP delamination from the concrete substrate. Li et al [16] studied the effect of the CFRP length and thickness on the stresses at the interface and how these affect the cracking pattern and failure mode. They noticed that bi-layer strengthening with CFRP sheets increased the beam stiffness compared to uni-layer strengthening similar to increasing the CFRP thickness. They also observed that debonding susceptibility decreases by reducing the CFRP thickness. A further experimental and numerical study by Bodin et al [19] showed that using two layers of FRP composites can lead to a significant

increase in both the ultimate capacity and the stiffness of the strengthened beams in comparison with using one layer of FRP composites. In their study, they have not noticed any delamination between the two layers of the FRP composites. However, the failure was by a propagation of a horizontal crack in the concrete cover.

There is no big difference between the performances of single or double layer strengthening for the initial cracking loads except that the cracking loads can be more improved in two layers than single layer. Furthermore, FRP tensile stresses are much smaller in two layers than in one layer.

Debonding propagation depends on the strength properties of the substrate and the interface. Debonding of the FRP reinforcement from concrete substrate is considered an important failure mode as it occurs at premature load levels causing a brittle failure [20]. Flexural or even shear cracks usually form at a load level less than the ultimate failure load of the beams. Under loading, cracks tend to open and will induce high shear stresses at the FRP-concrete interface [21, 22]. Therefore, debonding can also initiate at cracks locations in the concrete substrate and propagate to end of the FRP strengthening plate. Generally, debonding failure type occurs in beams reinforced with FRP that are short and brittle in nature.

Table 1 explains a summary of all the existing experimental works mentioned above. In some situations, it is necessary to strengthen RC beams due to some reasons by attaching one layer of FRP to the soffit of the beam. As known, increasing the FRP width would cause a regulation of the stress's distribution. But increasing the FRP thickness layers would cause a debonding. To the author's knowledge, how debonding increases significantly with increasing FRP thickness has not yet been studied theoretically only with few experimental studies that directly explain this information.

Table 1: Summary of existing experimental work

Researcher	Type of sample test	Specimen dimensions; L×b×h (mm)	Number of samples	Strengthening with FRP
Oehlers and Moran [11]	simply supported over the two edges	Different geometry and material properties	57	Single CFRP attached to the beams but with different lengths, widths and thicknesses
Li et al. 2006 [16]	Four-point bending test on simply supported beams	2000×120×200	7	Single layer strengthening and double layer strengthening, and three lengths of CFRP, i.e. 0.6, 1.2 and 1.6 m are considered.
Harajli and Soudki 2003[17]	simply supported over the four edges	670 × 670 × (55,75) slab and a 100×100 centre column stub	16	CFRP sheets bonded orthogonally and in one or two layers
Garden et al. 1997[18]	Four-point bending test on simply supported beams	1000×100×100	18	Single CFRP attached to the beams but with different lengths and thicknesses
Bodin et al [19]	Four-point bending test on simply supported beams	3000×150×300	7	1.2 mm thick and 5 cm wide CFRP plates. One layer of two plates or two layers of two plates

Many researchers studied increasing the thickness of the FRP experimentally, but none of them studied how that increase affects debonding. This paper explains the interfacial slip profile of the adhesive layer between the concrete surface and the CFRP sheets and tensile strain profiles along CFRP.

From the above discussion, it is evident that there is limited research on the effectiveness of the thickness of the externally bonded FRP sheets in strengthening RC beams. This study is carried out to examine the effect of increasing FRP thickness in the strengthening of reinforced concrete beams. Experimental results are presented and discussed and the shear strength data are calculated based on the numerical results.

2- Research significance

FRP composites have been used to strengthen RC beams in order to improve their structural performance by the transmission of shear and normal stresses at the plate-concrete interface, especially in the material discontinuities. Based on that, many structural members are intended to be strengthened with the belief that increasing the FRP thickness could increase the total ultimate capacity of the member. This study introduces an important explanation about the FRP-concrete interface, and how failure takes place during loading. Furthermore, it gives a prolong explanation about using one layer or multilayers of FRP in strengthening with a final judgement. Finally, the mechanism of failure is explained briefly.

3- Methodology of the research

This research paper explains how debonding of FRP composites increases with increasing FRP thickness in RC beams externally strengthened with FRP composites. Firstly, an experimental programme conducted by Obaidat et al [23] was chosen, and a full description of the study was introduced. In this model, two beams, unstrengthened (RF) as the control beam and strengthened (RF2) both have a rectangular cross section of 150 mm width and 300 mm height with a total length of 1960 mm are studied. The beams were simply supported with a total span between the supports is 1560 mm. The beams were tested experimentally under Four-point bending test on simply supported beams where the total load is applied to two point loads that divide the length between supports to three equal parts of 520 mm as shown in Figure 1 below.
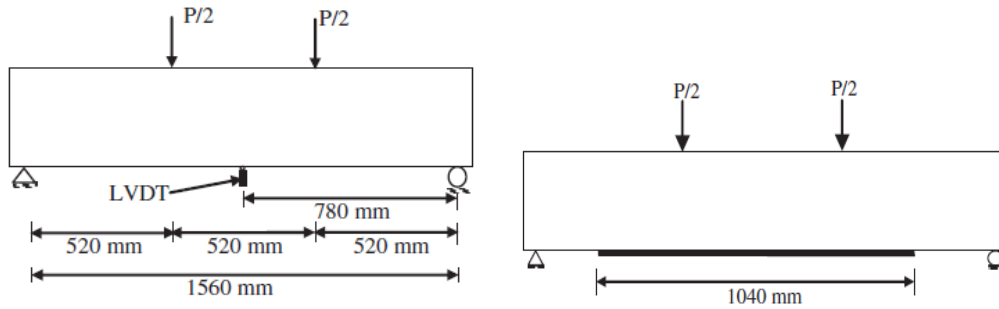
Figure 1: Schematic of the control and strengthened beams in the experimental work [23]

The beams were reinforced in flexure with 2Ø12 mm and the compression reinforcement was 2Ø10mm as shown in Figure 2 below.
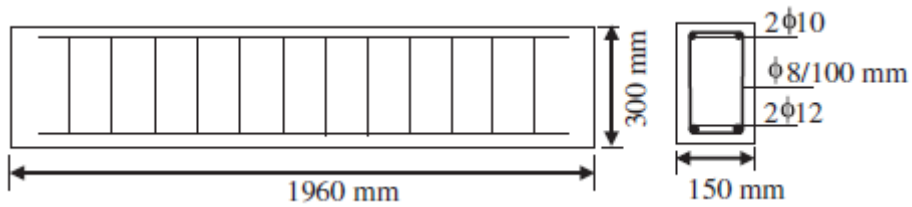
Figure 2: Beam reinforcement details [23]

Both the flexural and compression reinforcement were tied together by 8 mm stirrups distributed at 100 mm along the whole beam length. The concrete cover to the flexural reinforcement was set to 25 mm in all the beams. The retrofitted beam was strengthened with externally bonded CFRP plate with a thickness of 1.2 mm and a width of 50 mm with a total length of 1040 mm. The CFRP laminate was applied along the longitudinal centre line at the bottom soffit of the beam as shown in Figure 3 below. Material properties for the concrete, steel bars, CFRP strips and the adhesives used in the experimental and the simulation are explained in Table 2 below.
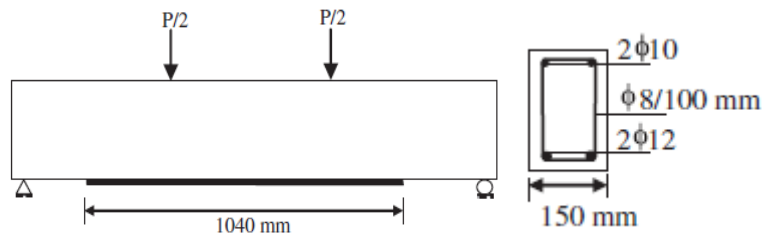
Figure 3: Schematic of the beam details with CFRP composites [23]

Table 2: Material properties of Obaidat et al beams

Material	Description	Value
Concrete	Elastic modulus, GPa	26
	Poisson ratio	0.2
	Characteristic compressive strength (f_c), MPa	29
	Characteristic tensile strength (f_t), MPa	1.81
Reinforcement		
Ø 8 mm	Not tested	Not tested
Ø 10 mm	Elastic modulus, GPa	211
	Poisson ratio	0.3
	Yield strength (f_y), MPa	520
	Ultimate stress, (MPa)	741
	Ultimate strain	0.151
Ø 12 mm	Elastic modulus, GPa	207
	Poisson ratio	0.3
	Yield strength (f_y), MPa	495
	Ultimate stress, (MPa)	760
	Ultimate strain	0.167
CFRP	Thickness, mm	1.2
	Longitudinal modulus (E_1), GPa	165
	*Transverse in-plane modulus($E_2=E_3$), GPa	9.65
	*In- plane shear modulus ($G_{12}=G_{13}$), GPa	5.2
	*out- of-plane shear modulus (G_{23}), GPa	3.4

	*Major in-plane Poisson ratio, $\nu_{12} = \nu_{13}$	0.3
	*Out-of-plane Poisson ratio, ν_{23}	0.45
	Characteristic tensile strength (f_t), MPa	2640
Epoxy adhesive	Compressive strength, MPa	40
	Thickness, mm	1.0
* Material properties are taken from Obaidat et al [24]		

Then, a 3D finite element model using ABAQUS 6.13 conducted a validation of the experimental work with the introduction to the suitable elements, material properties, damage initiation and evolution, and failure criteria. Finite element modelling was performed by the explicit procedure as a quasi-static solution by the Concrete Damage Plasticity model. All the material properties were taken from Table 2 above. The load was applied as a uniform pressure over a steel bearing plate of a width 100mm on the top surface of the beam as in the experiment. Due to the symmetry, a quarter of the beam was modelled in order to reduce the computer time consumption. Figure 4 shows the FE model of the simply supported CFRP-strengthened RC beam.
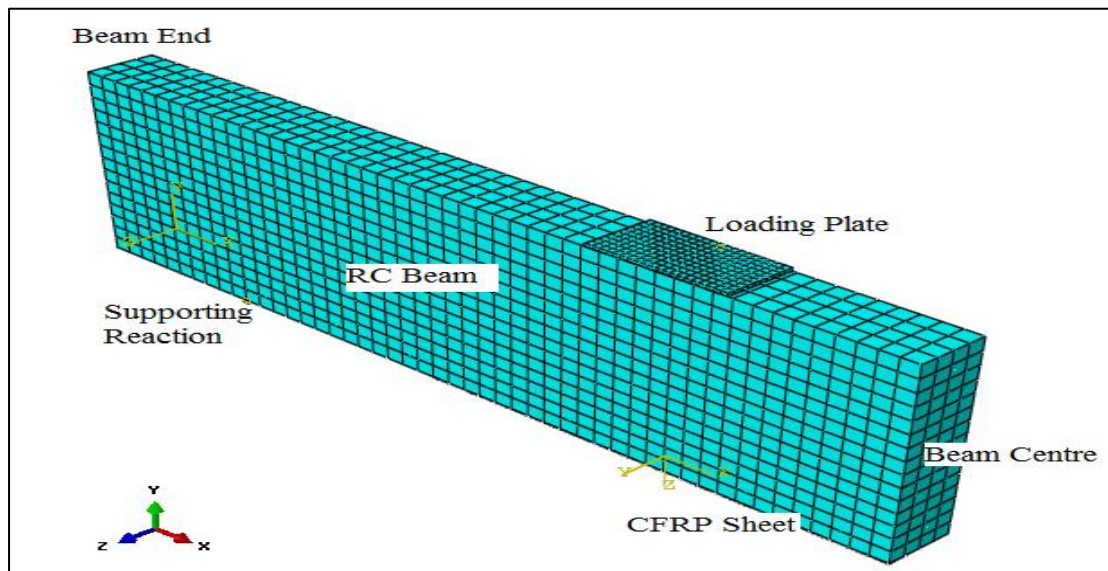
Figure 4: Quarter of the RC beam adopted in the FE modelling

Further study was conducted based on the validated model on the interfacial slip profile of the strengthened RC beam and the tensile strain profile along the CFRP composite. Furthermore, an additional numerical study was conducted on the effect of adding two layers of CFRP composites for strengthening beams and how that affect the failure mechanism. Finally, some conclusions were drawn based on the study. Figure 5 shows a flowchart explains the steps conducted in this paper.

Introduction to the subject and literature review of all the previous studies related to the using of FRP composites in strengthening RC beams

Methodology of the research in which experimental work and the numerical study were explained in detail. Dimensions of the tested beams, properties of all the material used in the test and how the numerical model was conducted were presented.

Numerical Model Validation in which all the elements and corresponding material behaviours were chosen

Results and discussions were introduced

Conclusions and recommendations to the conducted research

Figure 5: Flowchart of the present study

4- Numerical Model Validation

Complex phenomena (like nonlinearity and failure) that are difficult to be explained experimentally can be explained based on numerical models. These models evaluate changes in experimental behaviour, and can explain the multiple steps that can occur and their influence on these phenomena.

Although experimental results can explain failure behaviour, some aspects of material strength; such as logarithmic strains at all positions of a cross section and nonlinear

stress profiles are not easily accessible due to insufficient instrumentation or the physical impossibility of positioning it. Therefore, a high level of instrumentation is required that causes increase in the cost of experimentation. Therefore, using numerical models makes it possible to evaluate these results at any node of the discretized model.

The general failure modes of the concrete compromise the crushing under compression and the cracking under tension stresses. The concrete failure process can be described by the irreversible deformations and the stiffness degradations that cause a decrease in the stresses with an increase in the concrete strain, which is called strain softening [25]. In order to get a reasonable solution for the concrete failure, it is important to select a constitutive model that has the ability to combine both the plasticity and damage. Concrete behaviour in ABAQUS is modelled by the damage-plasticity model, which is able to give suitable and reasonable results for the numerical simulation of the concrete crushing, cracking and the CFRP-concrete interface debonding [25, 26].

The Concrete Damage Plasticity model available in ABAQUS is used in models here to validate with the experimental results. Based on the results of the uniaxial compression test that can be conducted on any concrete section, the stress-strain relation can be accurately described. The concrete response is linear up to the initial cracking, then it is characterised by the stress hardening up to the maximum compressive stresses. Then, a strain softening occurs up to the failure. ABAQUS needs to define both the stress hardening and strain softening as a compressive stress (σ_c) and inelastic strain (ε_c^{in}). For the compression behaviour, the stress-strain relationship described by Eurocode 2 [27] was adopted in this study as explained in Figure 6.
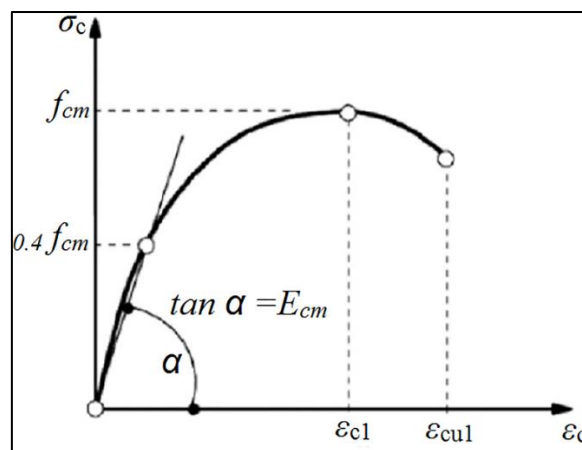
Figure 6: Uniaxial stress-strain curve for concrete [27]

When tensile stresses are applied to a concrete section, cracks occur at locations where the tensile strength is violated. Nevertheless, concrete between cracks is still able to carry tensile stress what is known as "tension stiffening or stress softening" [28]. Using stress-strain approach in the stress softening can cause mesh sensitivity which means the divergence of the analysis when the mesh refined due to the formation of narrower cracks rather than the formation of additional cracks [29]. The tensile behaviour was based on the exponential relationship between the tensile stresses and the concrete crack width described by the equation of Cornelissen et al [30] as shown in Figure 7.
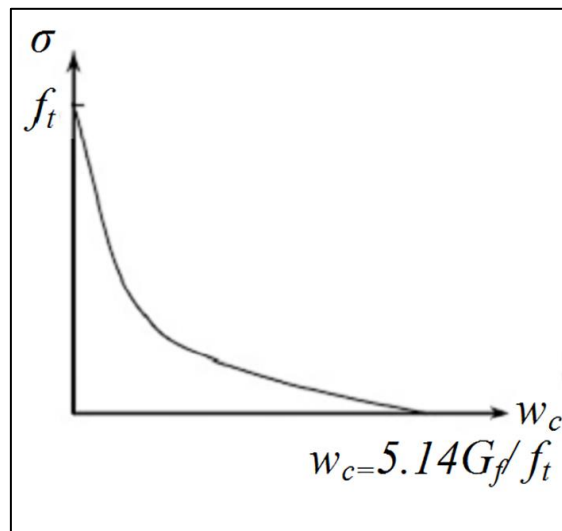
Figure 7: Exponential tension stiffening curve [30]

$$\frac{\sigma}{f_t} = f\left(\frac{W}{W_c}\right) - f(W_c) \dots\dots\dots\dots\dots\dots\dots\dots\dots\dots\dots\dots\dots\dots\dots\dots\dots\dots\dots\dots..\dots\dots\dots..(1)$$

$$f(w) = \left[1 + \left(\frac{C_1 W}{W_c}\right)^3\right] exp\left(\frac{C_2 W}{W_c}\right) \dots\dots\dots\dots\dots\dots\dots\dots\dots\dots\dots..\dots\dots\dots\dots..(2)$$

Where C_1 and C_2 are 3 and 6.93 respectively for normal weight concrete [30].

Modelling the interaction between the steel reinforcement and the concrete in the finite elements is the most difficult and controversial aspect as many models are able to simulate the experimental behaviour without taking in consideration the effect of bond-slip [31]. Furthermore, other factors like the chemical adhesion and friction between the concrete and steel bars may play a big role in the behaviour. Therefore, the modelling is extremely complex. And thus, the reinforcement mesh was embedded

through the concrete elements with full bond between the two. Embedded region constraint was used to model the steel-concrete interface. Embedding means that the translational degree of freedom at the node in the reinforcement element is eliminated by constraining it to the interpolated value of the corresponding degree of freedom in the host solid element [32]. When an embedded node is positioned near the edge or face of the host element, this node makes a small adjustment to its position in order to precisely lie on the edge or face of the host element. In this way, an embedded element may share some nodes with the host element and a perfect bond can be assumed between host and embedded elements. The reinforcement mesh consists of three dimensional 2-nodes truss elements (T3D2). Structural effects that are associated with the bond between the concrete and the steel bars, like the tension stiffening, bond-slip and dowel action, are tacitly considered in ABAQUS by modifying some aspects of the plain concrete to imitate them [32]. The structural behaviour of steel bars is defined based on the stress-strain results of the uniaxial tensile tests and the results from Table 2 above. The elastic behaviour is characterised by the Young's modulus and Poisson's ratio, while the inelastic behaviour is characterised by the data pairs of true stress and true plastic strain. Figure 8 shows the embedded steel reinforcement in the concrete (host) elements.
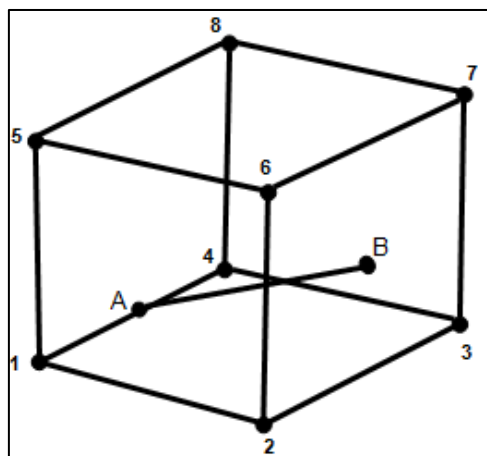
Figure 8: Truss element AB embedded in (3-D) continuum element; node A is constrained to edge 1-4 and node B is constrained to face 2-6-7-3 [32]

The CFRP plates are unidirectional and have similar properties in any direction perpendicular to the fibres direction. The composite strip failure is defined based on a stress-based failure called Hill-Tsai failure theory and the strips can be considered as

transversely isotropic and the stiffness parameters are five [33]. Continuum 2D shell elements (S4R) were used to model the CFRP material based on Table 2.

There are two different types of the adhesive modelling techniques in the ABAQUS. The first type is defining the adhesive as a material property using adhesive elements. The second type is surface based interaction property [34]. In this study, the interface is modelled by using surface-based contact and a cohesive behaviour is defined through the study as interaction properties. The constitutive response of the cohesive surface interaction approach depends on traction-separation-based response. The general formulas and the constitution laws of surface-based cohesive behaviour are very similar to the cohesive element in which they require a linear elastic traction-separation, damage initiation criteria and damage evolution low.

In order to get an exact structural behaviour when the bond between the concrete and the FRP is considered, these three parameters are discussed in deep.

Failure criteria:
The traction-separation model in ABAQUS assumes a linear elastic behaviour followed by the initiation and evolution of the damage as shown in Figure 9 [33]. The initial stiffness parameters assume same and are linear in all directions until the initiation of damage. The traction-separation model was used with specified mechanical and geometric parameters to capture the failure of contact. These parameters include initial stiffens (K_0), shear strength (τ_{max}), and fracture energy (G_f). The traction-separation parameters can be expressed according to following equations [23]:

$$K_0 = \frac{1}{\frac{t_a}{G_a} + \frac{t_c}{G_c}} \dots\dots\dots\dots\dots\dots\dots\dots\dots\dots\dots\dots\dots\dots\dots\dots\dots\dots\dots\dots\dots\dots\dots\dots\dots\dots\dots (3)$$

Where t_c is the thickness of concrete; t_a is the thickness of adhesive; G_c is the shear modulus of concrete; G_a is the shear modulus of adhesive.
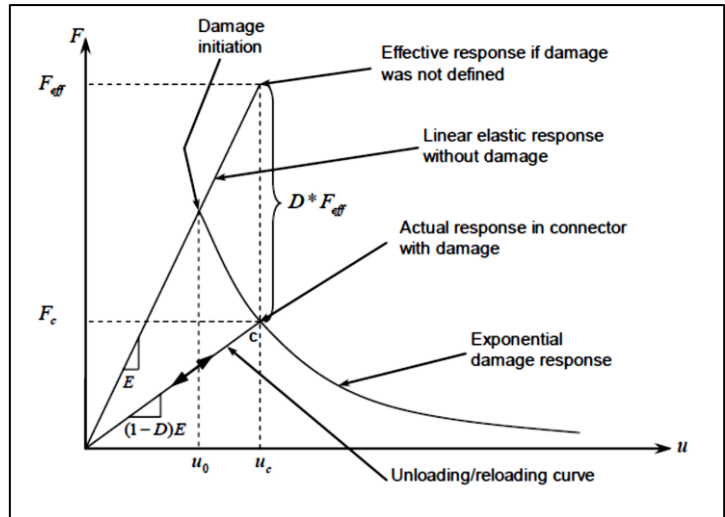
Figure 9: Exponential damage evolution [35]

The debonding between the FRP and the concrete substrate occurs when either the interface shear stress ($t^0{}_s$ or $t^0{}_t$) or the effective displacement at damage initiation (S_0) is violated. When a sufficient bond length is provided, the failure takes place around the load application region and moves to the plate ends. But, when insufficient bond length is provided, debonding starts at the plate ends and moves towards the whole plate [35]. A linear ascending branch was adopted for the simplicity of data entry into the FE model. The model is given as follows:

$$\tau = \tau_{max} \frac{S}{S_0} \quad if\ S \leq S_0 \dots\dots\dots\dots\dots\dots\dots\dots\dots\dots\dots\dots\dots\dots\dots\dots\dots\dots. \ (4)$$

$$\tau = \tau_{max} e^{-\alpha\left(\frac{S}{S_0}-1\right)} if\ S > S_0 \dots\dots\dots\dots\dots\dots\dots\dots\dots\dots\dots\dots\dots\dots \ (5)$$

The maximum shear stress τ_{max} (MPa) is governed as stated previously by the concrete tensile strength, f_t (MPa), and the FRP width ratio, β_w , and taken as follows:

$$\tau_{max} = 1.5\beta_w f_t \dots\dots\dots\dots\dots\dots\dots\dots\dots\dots\dots\dots\dots\dots\dots\dots\dots\dots. \ (6)$$

Where β_w is taken as follows:

$$\beta_w = \sqrt{\frac{2.25 - \frac{b_f}{b_c}}{1.25 + \frac{b_f}{b_c}}} \dots\dots\dots\dots\dots\dots\dots\dots\dots\dots\dots\dots\dots\dots\dots\dots\dots\dots. \ (7)$$

Where b_f, b_c, are the widths in mm of the FRP and concrete substrate respectively. The slip S_0 depends on f_t (MPa) and β_w as well and can be taken as follows:

$$S_0 = 0.0195\beta_w f_t \text{ in mm} \dots\dots\dots\dots\dots\dots\dots\dots\dots\dots\dots\dots\dots\dots\dots\dots\dots\dots (8)$$

The factor in equation (5) is related to the interfacial fracture energy (the energy required to introduce a unit area of interfacial-bond crack), as follows:

$$\alpha = \cfrac{1}{\cfrac{G_f}{\tau_{max}S_0} - \cfrac{2}{3}} \dots\dots\dots\dots\dots\dots\dots\dots\dots\dots\dots\dots\dots\dots\dots\dots\dots\dots\dots (9)$$

$$G_f = 0.308\beta_w{}^2\sqrt{f_t} \dots\dots\dots\dots\dots\dots\dots\dots\dots\dots\dots\dots\dots\dots\dots\dots\dots (10)$$

Damage initiation:

It is the beginning of the degradation in the material when the failure criterion is violated [36]. The high sensitivity of the damage initiation to the strain and displacement makes stress-based criterion give a more accurate damage prediction [6]. In this study, the damage initiation criterion is assumed to be violated when a quadratic interaction function reaches a value of one. This criterion can be represented as:

$$\left\{\frac{\langle t_n \rangle}{t^0{}_n}\right\}^2 + \left\{\frac{t_s}{t^0{}_s}\right\}^2 + \left\{\frac{t_t}{t^0{}_t}\right\}^2 = 1 \dots\dots\dots\dots\dots\dots\dots\dots\dots\dots\dots\dots\dots\dots\dots (11)$$

Where t_n represents the nominal tensile strength that causes failure (usually the tensile strength of the concrete, as the failure occurs in the concrete not in the adhesive). Furthermore, owing to the isotropic nature of the adhesive material, t_s, t_t are also used equal to t_n [34].

Damage evolution:

It describes the rate at which the material stiffness is degraded once the initiation criterion is violated and in this study it is assumed to be exponentially based on Lu et al [37] model. In ABAQUS, the damage evaluation was specified as a mixed mode function using mode-independent fracture model available in ABAQUS library with a

mode mix ratio of traction. The response is characterised as a tabular function of the difference between the relative motions at ultimate failure and the relative motions at damage initiation $(u_c - u_0)$, while the damage variables are calculated based on equation 12 below:

$$D = 1 - \left\{ \frac{\delta_m^0}{\delta_m^{max}} \right\} \left\{ 1 - \frac{1 - exp\left(-\alpha \left(\frac{\delta_m^{max} - \delta_m^0}{\delta_m^f - \delta_m^0} \right) \right)}{1 - exp(-\alpha)} \right\} \quad\dots\dots\dots\dots\dots\dots\dots\dots (12)$$

Where δ_m^0 is the slip corresponding to the maximum shear stress as calculated by equation (8); δ_m^{max} is the maximum slip as calculated previously; α as calculated by equation (9).

The damage variable D represents the degradation in the stiffness of a material. It initially has a value of 0 and it is monotonically evolves from 0 to 1 upon further loading after damage initiation.

The Concrete Damage Plasticity model, which is suitable for reinforced concrete beams, is studied here, however the adhesion between CFRP composites and the concrete substrate has some complexity. The reason behind that is the fact that the material properties of the adhesive are often unknown, or the thickness is very small and can be considered "zero" in modelling. In ABAQUS, the traction-separation constitutive law relates the stresses to separations in the thickness and transverse shear directions is employed [32]. The cohesive elements carry loads to constrain the CFRP to the concrete substrate until loads and deformations on the cohesive elements cause damage and failure. When the element has fully failed, it will release an amount of energy equal to the critical fracture energy obtained from material tests. In the finite elements, the cohesive material must have finite definitions of stress and separation over which the fracture energy can be released. The material properties are such that the initiation of damage takes place when the slip between the concrete and the CFRP sheet reaches the effective displacement at damage initiation of $S_0 = 0.038mm$; but the final debonding takes place at a slip $S_f = 0.762mm$ based on Lu et al [37] model for the calculation of bond-slip properties of CFRP-Concrete interface. The numerical study resulted a fracture energy as about 501J/m^2.

The thickness of the cohesive material was defined by the geometric thickness as zero and then to manually define a constitutive thickness.

Figure 10 shows a schematic representation of the procedure for the development of the traction-separation approach used in this study.

Creating both the cohesive zone and the FRP sections along with the RC beam, reinforcement, and loading and support sections.

Creating the mechanical behaviour of the FRP-concrete interface based on elastic traction type with:
E=26GPa , G1=7.8GPa , G2=7.8GPa

Creating the damage of the cohesive zone based on the traction-separation model with maximum quadratic stress damage:
Nominal stress normal-only mode= 1.81 MPa
Nominal stress first direction=2.986MPa
Nominal stress second direction=2.986MPa

Creating the damage evolution as:
Type =displacement
Softening=tabular
Degradation=maximum
Mixed mode behaviour=mode-independent
Mode mix ratio=traction
All the damage variables are taken from equation 12, while the displacements are characterised as a tabular function of the difference between the relative motions at ultimate failure and the relative motions at damage initiation

Figure 10: schematic representation of the procedure for the development of the

traction-separation approach

For the modelling of FRP-concrete interface, a predefined bond-slip model relationship is considered, and thus, the debonding is considered as the failure of the interface elements. So, choosing an accurate bond-slip model can give accurate results. The general contact algorithm in ABAQUS/Explicit uses balanced master-slave weighting whenever possible. A surface-to-surface contact interaction is used and implemented in the current study. The contact interactions are defined by specifying surface pairing in ABAQUS model. In this study, a mechanical contact interaction with a frictionless tangential behaviour was chosen in which the contact between the surfaces is frictionless. Furthermore, a mechanical contact pressure-overclosure relationship referred to as the "hard" contact model is chosen in the normal direction to resist the penetration. Figure 11 shows a diagrammatic representation of the model in which the details of the contact pairs are presented. Furthermore, Figure 12 shows the contact properties used in both the tangential and normal directions in the current study.
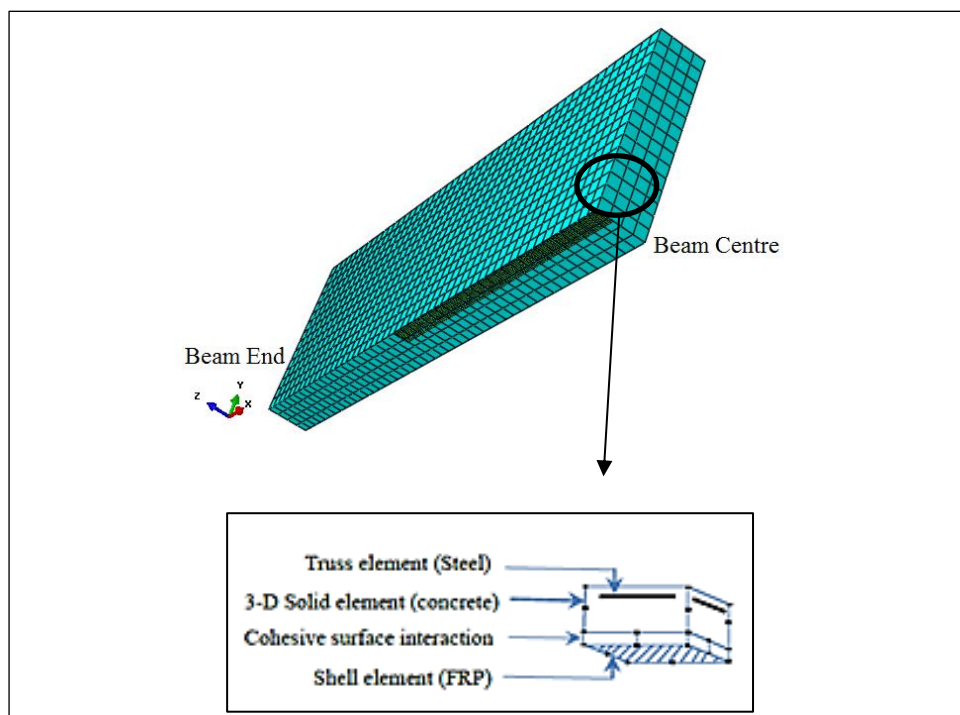
Figure 11: Finite element mesh of the quarter of CFRP strengthened beam
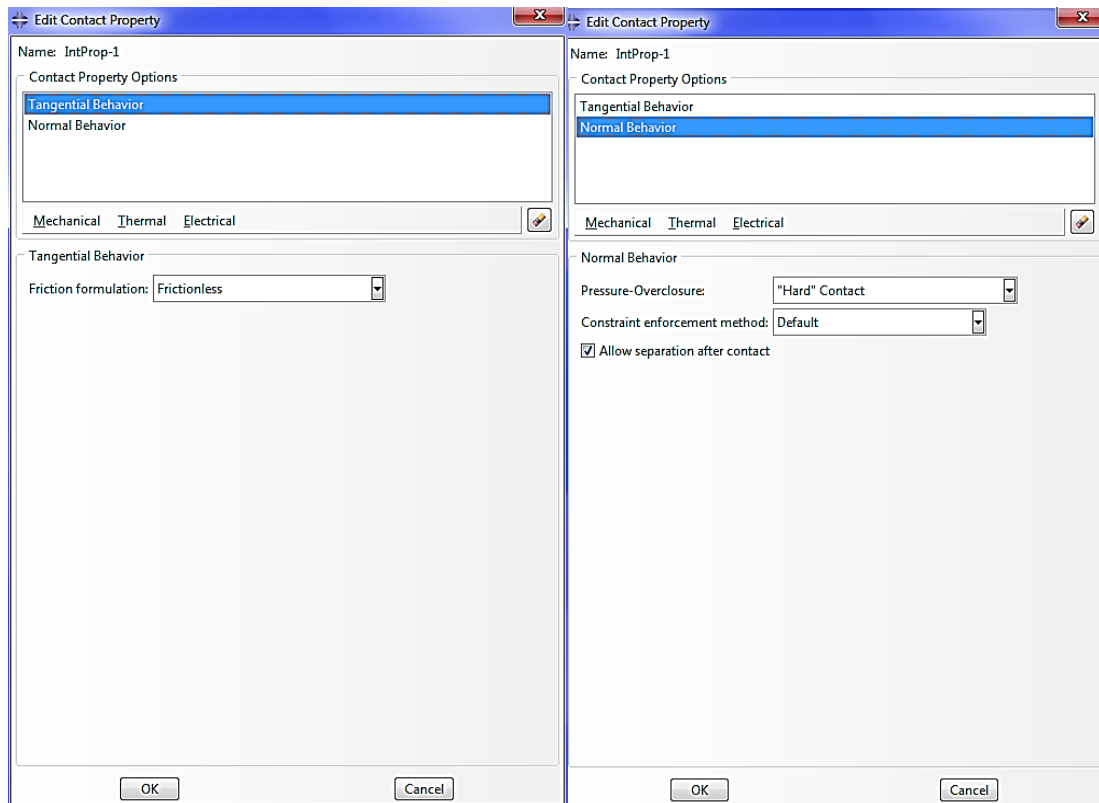
Figure 12: Contact properties used in both the tangential and normal directions

The bond between the CFRP and concrete and the both CFRP layers was modelled using cohesive elements (COH3D8) with the adhesive layer being modelled using a single layer of cohesive elements. Debonding of the CFRP strips is represented by the onset of damage in the cohesive elements [32, 37]. Damage initiation is defined using a maximum nominal stress criterion as described by [37, 38, 39, and 40].

5- Results and discussions

5.1 Validation of the Numerical Model to the Experimental Results

The first step to validate the numerical model to the corresponding experimental results is conducting a mesh sensitivity study. In this study, it is required to find an element size that gives the best fitting and will not give any change in the results with decreasing, or increasing, the element size. Based on a mesh sensitivity study (not presented here), it was found that a mesh with an element size of 20 mm was the most efficient arrangement can giving an acceptable level of accuracy with low computational expense. Figure 13 shows the comparison between the numerical and the experimental results for both the control and the retrofitted beams. It can be seen that there is a good agreement between them.
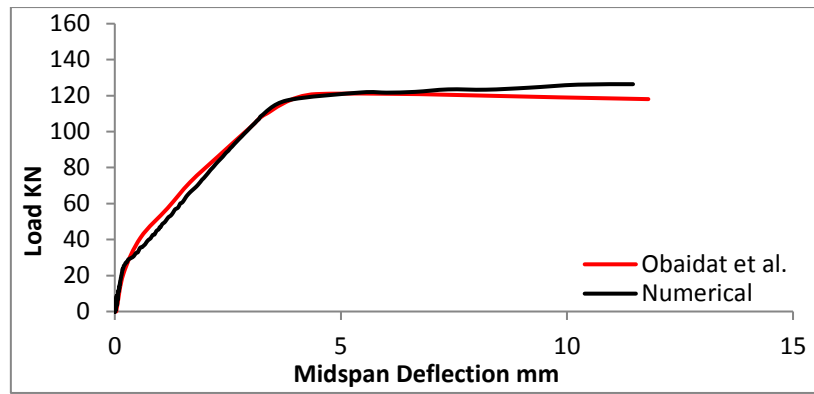
(a) Control beam
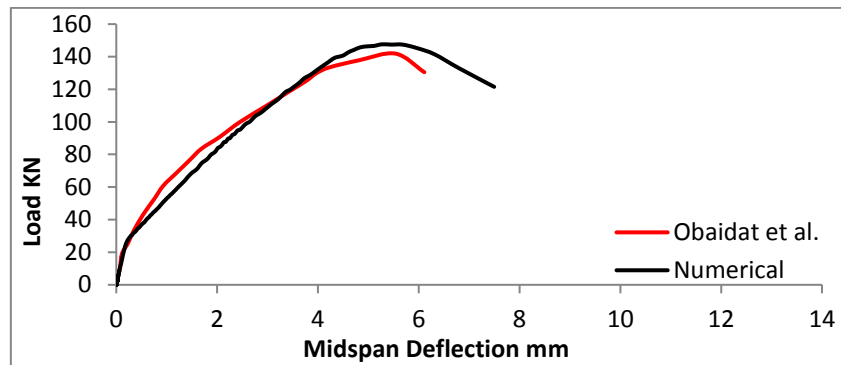
(b) Retrofitted beam

Figure 13: Load versus midspan deflection

In both the experimental and numerical studies, the unstrengthened beam (RF) behaved in a ductile manner and with failure characterised by yielding of the flexural reinforcement and the formation and widening of flexural cracks around the mid-span. The concrete damage plasticity model adopted in the finite element model used in ABAQUS does not directly show the direction of the cracks, but it assumes that the direction of the vector normal to the crack plane is parallel to the direction of the maximum principal plastic strain in concrete [32]. Figure 14 shows the experimental cracking pattern and the corresponding maximum principal plastic strains in the numerical model for both the unstrengthened and strengthened beams.

The strengthened beam (RF2) in the experimental and numerical studies experienced a brittle failure due to the sudden debonding of the CFRP plate from the concrete substrate at ultimate load. This was due to the concentration of the high shear stresses at the discontinuities of the CFRP plate.
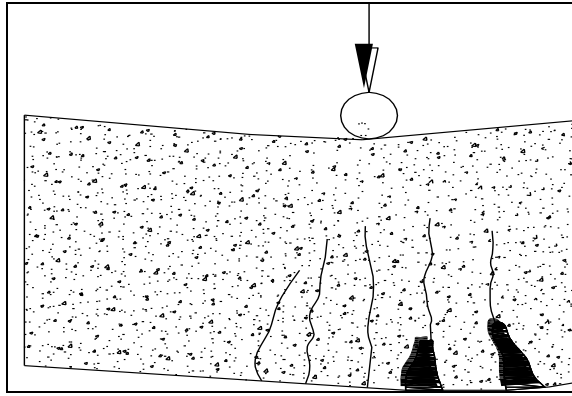
    (a) Control beam experimentally   (b) Quarter of the control beam
         numerically
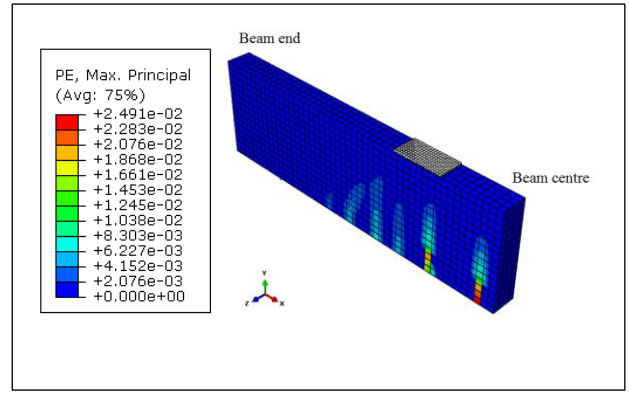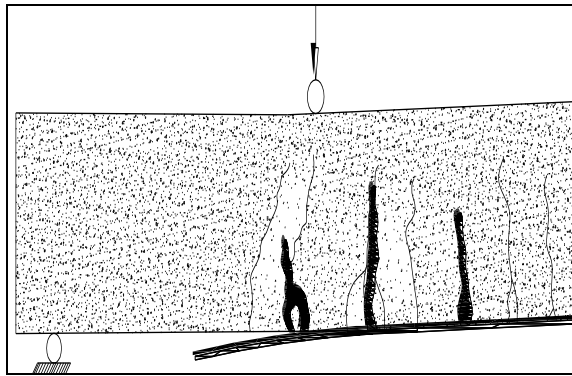
(c) Strengthened beam experimentally   (d) Quarter of the strengthened beam
numerically
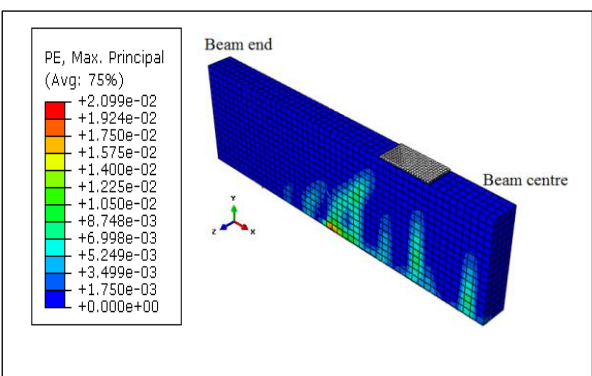
Figure 14: Crack pattern (left) and numerical plastic strains (right) at failure

There is a difference between the crack propagation and the final crack pattern for both the control and the strengthened beam. There are few flexural cracks with large width in the control beam, while in the strengthened beam there are many flexural cracks with smaller width. This is due to the confinement of the cracks by the CFRP plates.

5.2 Interfacial slip profile

In all the existing bond-slip models, the shear displacement is taken to be the relative displacement between the FRP plate and the concrete substrate [22]. Before debonding, the shear displacement results from the deformation of the adhesive itself. While after debonding, shear displacement includes the relative displacement between the two surfaces mentioned above. In all the models, it is assumed that the FRP plates carry the tensile stresses and the adhesive carries the shear stresses only.

The adhesive layer between the concrete surface and the CFRP sheets is modelled by using cohesive elements as presented previously. The behaviour of the interface is modelled based on the Lu et al [36] bond-slip model. In this model, damage is initiated when either interface shear stress (t^0_s or t^0_t) or the effective displacement at damage initiation (S_0) is violated. In this study, the damage is evaluated based on the difference in the horizontal displacement between two adjacent nodes of concrete elements and the CFRP elements and compared to the effective displacement at damage initiation.

The material properties are such that the initiation of damage takes place when the slip between the concrete and the CFRP sheet reaches the effective displacement at damage initiation of 0.038 mm; but the final debonding takes place at a slip of 0.762 mm based on Lu et al [37] model for the calculation of bond-slip properties of CFRP-Concrete interface. Figure 15 shows the change in the slip between the concrete and CFRP sheet after the initiation of damage at 56.92 kN in the strengthened beam RF2. It is noticed that the debonding occurs suddenly at the plate end at maximum load as in the experimental test. Increasing load application causes an increase in the slip profile due to the gradual loss of the stiffness in the concrete. The slip was observed to vary from the beam centre toward the plate end.
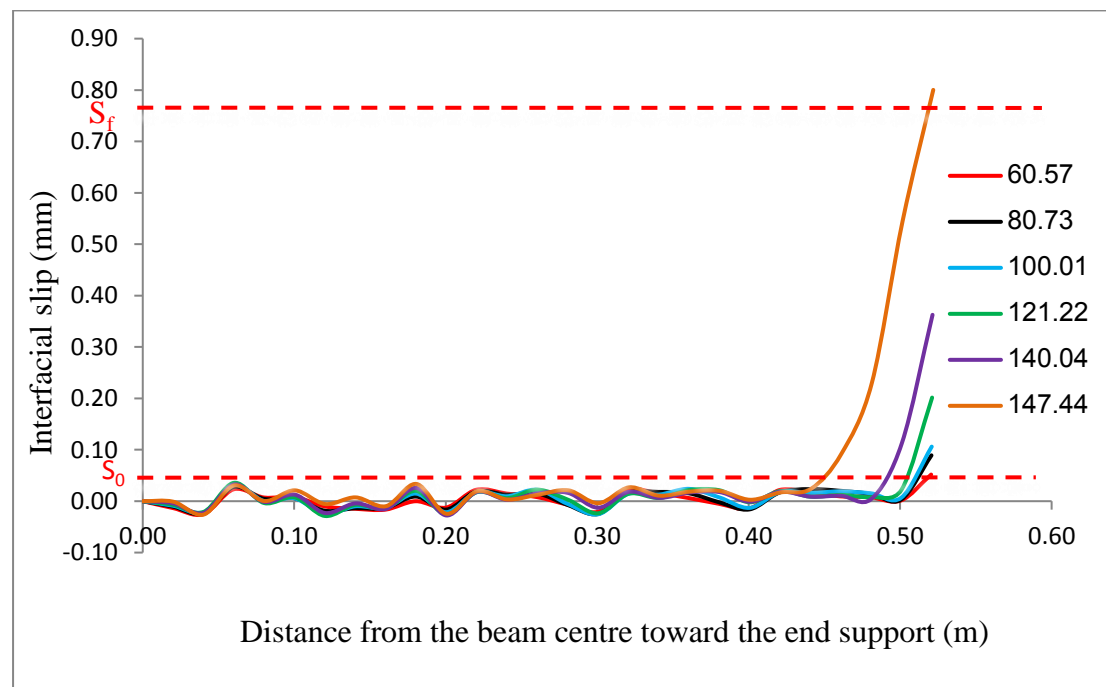
Figure 15: Numerical model: Comparison of slip profile at different load levels

Figure 16 shows the cohesive layer at the initiation of damage at load 56.92 kN and at the final debonding at the maximum load of 147.44 kN in the strengthened beam RF2. From the figure, it can be seen that the initial effective displacement was violated at the plate end due to the concentration of shear stresses, but the debonding was initiated at both the plate end and the flexural cracks region due to concrete cracking.
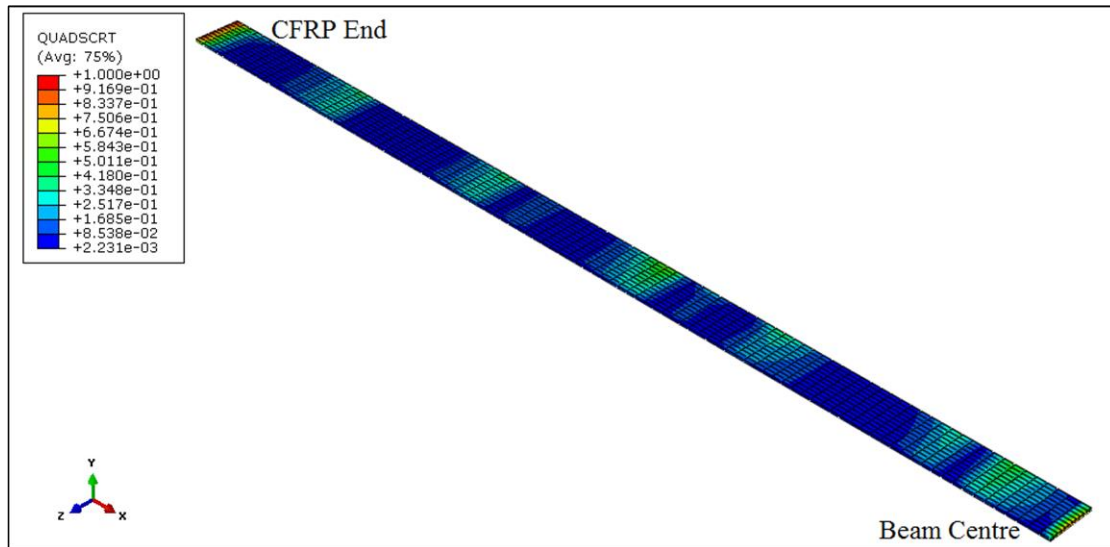
(a) Cohesive layer at damage initiation
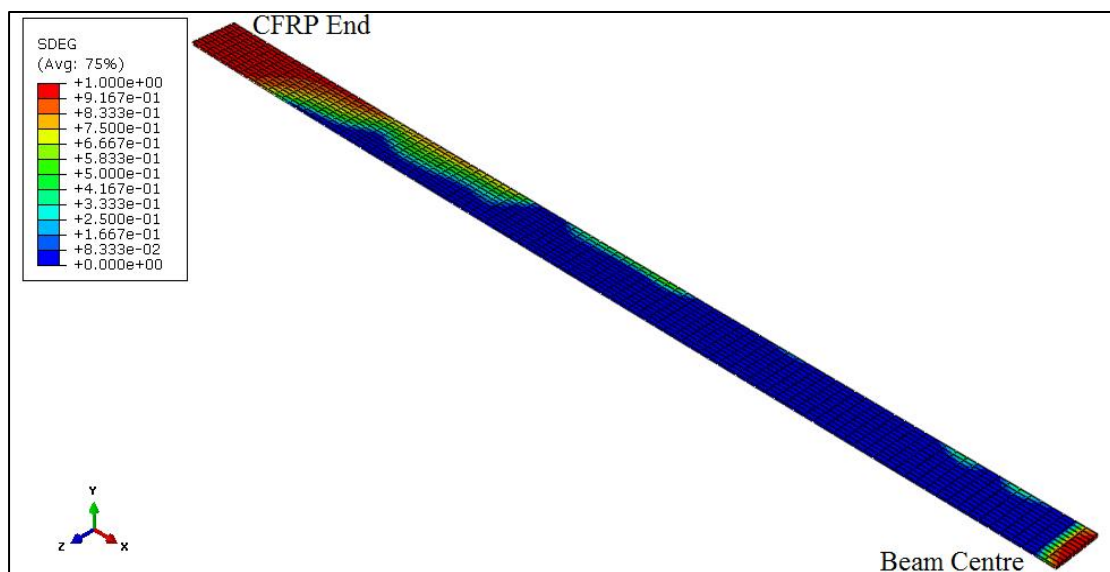
(b) Cohesive layer at final debonding

Figure 16 Cohesive layer at damage and debonding

When cracking occurs, the axial force in the concrete section cannot be sustained by the beam section. So, this force is transmitted to the CFRP plate through the cohesive layer causing shear stresses in the layer. The increase of this shear stress can cause the

debonding in the CFRP plate. Figure 17 shows the debonding in the CFRP plate at the plate end and mid-span of the beam in both experiment and FE model.
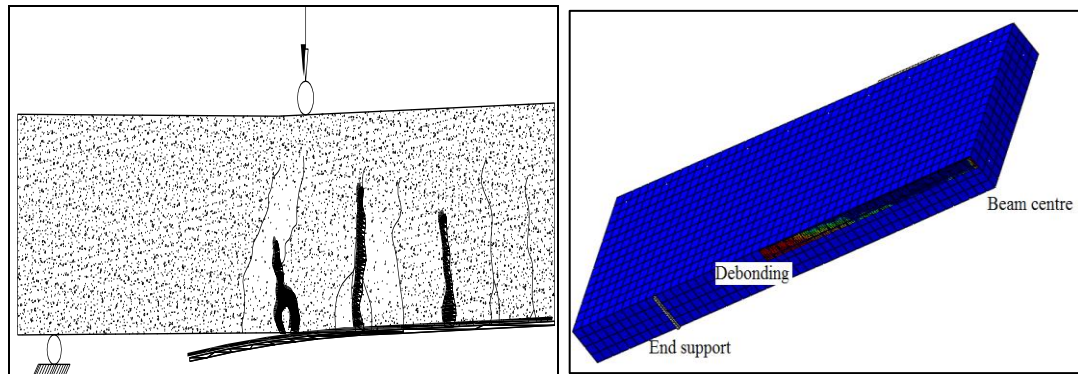
(a) Debonding failure in experiment   (b) Debonding failure in FE model

Figure 17: Debonding failure in the beam

5.3 Tensile strain profile along CFRP

Figure 18 shows the tensile strain profile along the CFRP sheet at four different load values after the initiation of damage in the cohesive layer between the concrete and the CFRP sheet. It can be seen that the strain profile has a reverse trend to the interfacial slip profile meaning high strains take place at low slip locations. It is also seen that the CFRP axial strain increases due to both the stress transfer from the concrete section and the increase in the bending moment. Within the maximum moment region (beam centre between the applied load), the increase in the strain is less pronounced and the peak value close to the mid-span is due to the stress concentration at the cracking region.
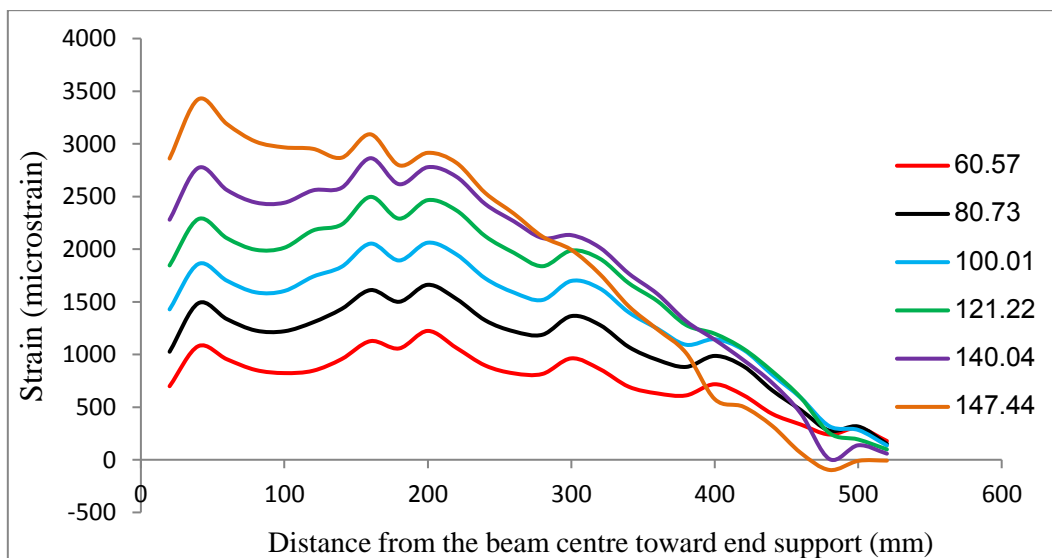
Figure 18: Strain profile along the CFRP sheet at different load levels

5.4 Adding two layers of CFRP in strengthening

In order to simplify the specimen's arrangement and to enable the reader to simply remember the thickness of the CFRP layer or the number of layers used in the study, specimens were renamed based on experimental or numerical study, strengthened or unstrengthened and number of layers used in the study. (E) means experimental study, (N) means numerical study, (U) means unstrengthened beam, (S) means strengthened beams. First number in the names refers to the thickness of the CFRP layer used in the study, while the second number refers to the number of layers used in the study. Table 3 explains a summary of the specimens tested in this study.

Table 3: Summary of the tested specimens in this study

specimen	Thickness of CFRP used	Number of CFRP used
Experimental Unstrengthened (EU-0-0)	0	0
Experimental Strengthened (ES-1.2-1)	1.2mm	One layer
Numerical strengthened (NS-1.2-1)	1.2mm	One layer
Numerical strengthened (NS-2.4-1)	2.4mm	One layer
Numerical strengthened (NS-1.2-2)	1.2mm	Two layers
Numerical strengthened (NS-0.6-2)	0.6mm	Two layers

After the numerical validation of the experimental study for both the unstrengthened and strengthened beams, an additional study was conducted with different CFRP thicknesses and layers. Two layers of 0.6mm thickness was used to give a total thickness similar to the thickness of one layer of 1.2mm which was studied numerically. By a comparison between this study and the experimental work, it is found that adding two layers similar to the thickness of one layer will not change the response of the beam. But, this will make the beam to behave with less ductility. Furthermore, the difference

between the two cases is; for one layer, debonding occurs at the free end and extends to the CFRP strip centre at the same time with debonding initiation at the strip centre. While, for the case of two layers, debonding at the strip centre does not occur only at the end strips and extends to the strip centre. This is similar to the case when insufficient bonding length is provided. During the simulation, no delamination was observed between the superimposed CFRP plates for the two layers of CFRP and the beam behaves as if the plate was thicker and no inter-layer delamination. An additional CFRP sheet with a thickness of 1.2mm is added over the previous one to give a total thickness of 2.4mm and a layer of cohesive elements was entered between them in order to check the effect of CFRP layers on debonding. Figure 19 shows the load-deflection curves for all the cases and how the ultimate capacity did not increase with increasing CFRP layers due to the debonding failure. It is also noticed that adding additional CFRP sheet reduced the total displacement of the beam and changed the failure mode to a sudden brittle failure. Figure 20 shows the change in the slip between the concrete and first CFRP sheet before and after the initiation of damage at 56.92 kN. It is noticed that the debonding occurs suddenly at the plate end at maximum load and transfers along the CFRP sheet towards the beam centre. No debonding occurs between the CFRP sheets due to the bonding adhesive strength is very large as compared to the concrete tensile strength. It is also noticed that using two layers of CFRP leads to a premature bond failure of CFRP due to the increased horizontal shear between concrete and CFRP as proved by the experimental work of Harajli and Soudki [17].
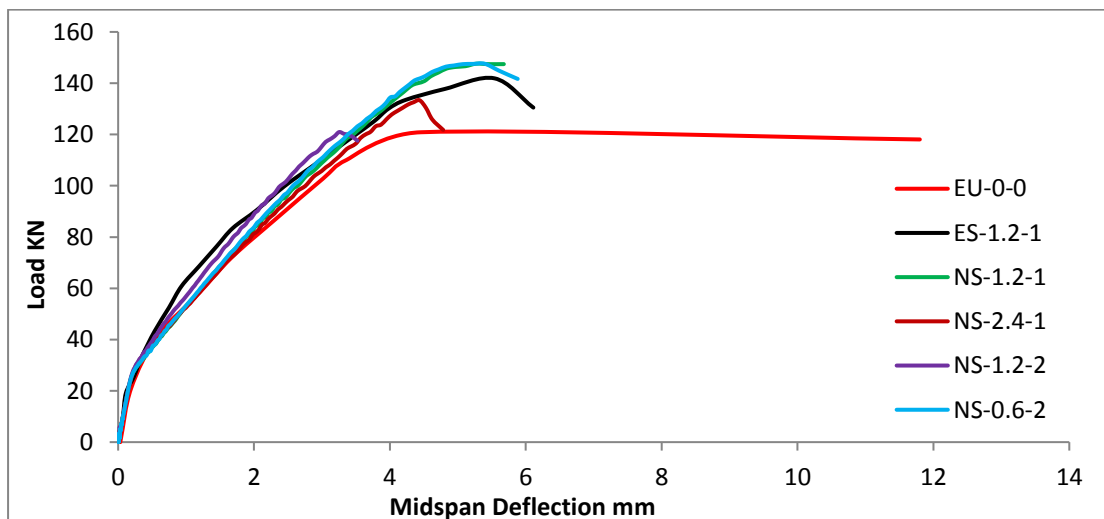
Figure 19: Load versus midspan deflection
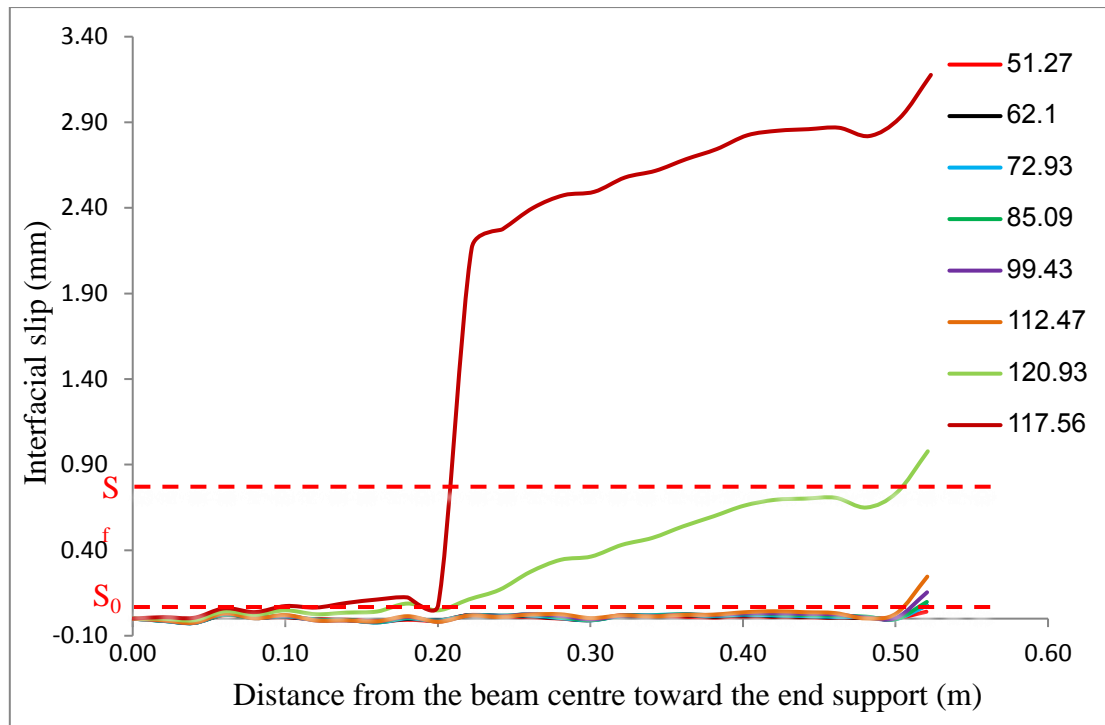
Figure 20: Comparison of slip profile at different load levels

A more interlaminar study shows that the steel tensile stresses are with small values for the two layers of 2.4mm total thickness. These stresses occur at the location of debonding only with a big stress at the stirrups in which within debonding region. While, for other cases, more stresses are found in the flexural reinforcement only at the location of debonding. Furthermore, the flexural reinforcement does not show a plastic strain in reverse to the other cases.

By checking the concrete stresses at failure, it is found that the beam has an irregular concrete compression stress at the case of two layers (2.4mm), and these stresses direct to the debonding location what causes a clear compression strut. In the case of one layer, a very clear compression strut occurs to the debonding region while for the case of two layers (1.2mm) there is no compression strut.

It is also noticed that using two layers of 1.2mm thickness CFRP gives less stresses at the debonding location than using two layers of 0.6mm thickness or even using one layer of 1.2mm thickness. Furthermore, the maximum stresses at the beam centre were noticed in the case of using one layer of 1.2mm thickness CFRP strip.

6- Mechanism of failure

A simple mechanical model for the FRP-concrete interface bonded joint can be established by assuming that the FRP plate and the concrete substrate are subjected to axial deformations only, while the interface is subjected to pure shear deformation. That is, all the bending deformations of both adherents are neglected and the shear stress across the thickness of the adhesive layer is constant. The adhesive layer in such a model is mainly subject to shear deformations.

In order to get more understanding on the interfacial stresses for the FRP-concrete interface, it is better to measure the shear stress for the FRP composites attached to the concrete substrate. The performance of the FRP-concrete interface in transferring stresses is of a crucial importance. However, the problem that arises when using this technique is the development of high interfacial shear stresses at the plate ends. These stresses are found by calculating the mean stress from the difference in the strain of two consecutive strain gauges [7]. The evaluation of the bonding shear-slip curve alone is not sufficient to provide data for providing a local interface law. The law depends also on the features of the adopted structural model [41]. There is a big difference between the models that experimentally and numerically calculated. For a member under experimental pure tension, slip must be referred to as an average displacement of the concrete cross-section. This thing is totally different with using finite elements discretisation. The interface law must be defined based on the adhesive thickness only. Thus, the interface is obtained from the deformations of both the FRP and the concrete substrate. Generally, experimental bond-slip curves are commonly calculated from a pull tests in two ways: (a) from axial strains of the FRP plates measured by closely spaced strain gauges; (b) from load displacement (slip at the loaded end) curves [37]. The first method does not give an accurate local bond-slip curves because the axial strains of the FRP plate have a variation as a result of the concrete cracks, concrete heterogeneity and the roughness of the underside of the debonded FRP plate. Strain gauges located over the cracks show a much higher strains than other gauges [22]. The strain difference became smaller with load increasing what means damage initiation along the interface. Consequently, different bond-slip curves can be found from different tests. The local bond-slip curves derived from the second method may lead to a similar load-displacement curves.

Based on the numerical analysis conducted in this paper, the debonding starts at the far end of the FRP plate. Thus, the maximum shear stress would be better calculated at that place. As known, FRP plates carry longitudinal stresses only while the adhesive carries the shear stresses only. So, the interfacial shear stresses are transferred through the shearing of the adhesive and are given by:

$$\tau = G\frac{(u_{FRP} - u_{Con.})}{h} \dots\dots\dots\dots\dots\dots\dots\dots\dots\dots\dots\dots\dots\dots\dots\dots\dots\dots\dots\dots (13)$$

Where G and h are the shear modulus and the thickness of the adhesive layer respectively; u_{FRP} is the longitudinal displacement of the FRP plate; and $u_{Con.}$ is the longitudinal displacement of the concrete.

Table 4 gives a comparison between the calculated shear stress of the four models based on the above equation. The numerical analysis showed that the shear stress of 1.2mm FRP thickness is less than that of 2.4mm FRP thickness. Furthermore, the damage of the FRP with 1.2mm thickness is concentrated at the FRP free end for a short distance. While, for the 2.4mm FRP thickness it is also at the free end but extended to a longer distance to the centre of the beam what causes earlier debonding. This confirms that increasing FRP thickness causes an increase in the interfacial shear stresses. Using two layers of FRP with 1.2mm thickness causes a reduction in the shear stress because the shear stress is calculated between the first FRP plate and the concrete substrate. Furthermore, it did not add any increase in the ultimate capacity but the beam failed with a brittle failure due to the sudden debonding of the CFRP plate from the concrete substrate at ultimate load. Using two layers of 0.6mm FRP thickness experienced a brittle failure due to the sudden debonding of the CFRP plate from the concrete substrate at ultimate load. As explained earlier, this was due to the concentration of the shear stresses at the discontinuities of the FRP plate. The values of the shear stresses for different models were presented in table 4 below.

Table 4: Calculated shear stresses for the computed models

Specimen	1.2mm FRP plate	2.4mm FRP plate	0.6mm FRP two plate	1.2mm FRP two plate	Lu et al equation
Shear stress	2.78 MPa	7.91 MPa	0.341 MPa	1.87 MPa	2.985 MPa

As explained previously, there is a difference between the defined shear stress in the model and the calculated one. The defined one represents the shear stress that already calculated based on Lu et al [37] equation in which the concrete tensile strength, fracture energy and the ratio of the FRP width to the concrete width is considered and represented in column 6 in Table 4 above. It is worth mentioning that the value of this shear stress is constant along the whole contact region in all the four models. The calculated shear stress was calculated on the location of the debonding takes place and it was on the free end of the FRP plate. Its value differs from the associated shear stress because it is calculated based on the FRP strains and the epoxy thickness.

The results of the numerical analysis show that the interface bond-stresses are non-uniformly distributed along the reinforced boundaries as it depends on the difference between the deformations of both the FRP and concrete as explained in equation (12), which was also mentioned by [4, 42]. Maximum shear stresses take place at the far end of the FRP where deboning is suspected to occur and reduce towards the beam centre. In particular, it is found that the shear stresses values exhibit peak values about 1 to 2 times greater than the mean values predicted by the classical beam theory.

7- Conclusions

The strengthening of reinforced concrete beams by externally bonded FRP strips has been used for more than two decades. The behaviour of such reinforced concrete beams was studied in this paper. It is well known that debonding increases significantly with increasing FRP thickness for a fixed FRP ratio. However, there is no theoretical study to explain how debonding increases with increasing FRP thickness and what happens within the bond between FRP and concrete. The followings can be concluded:

❖ Shear stress calculated in the FRP-concrete interface for a specific FRP thickness is less when the FRP composite thickness is doubled. This means increasing the FRP width is better than increasing its thickness for a specific FRP composite area.

❖ For a small FRP thickness, the damage is concentrated at the FRP free end and extends to a small distance only. Increasing the FRP thickness causes extension in the damage to a longer distance towards the beam centre and leads to an earlier debonding.

❖ Using two layers of a small thickness of FRP composites does not affect the total behaviour of the strengthened beams except for a reduction in the total ductility of the beam.

❖ Using two layers of a large thickness of FRP composites accelerates the debonding failure due to the increase in the horizontal shear between the CFRP sheet and the concrete section.

❖ Using one layer of FRP composite improved the ultimate capacity of RC beams by 22%, while using two layers does not increase the ultimate capacity of the beam, but the beam failed with a brittle failure due to the sudden debonding of the FRP composite. This is also related to the reduction in the shear stress value.

❖ Adding one layer of CFRP causes debonding to occur at the free end and extends to the FRP centre at the same time with debonding at the strip centre.

❖ Adding two layers of FRP causes debonding at the free ends only and then extends to the strip centre.

❖ This study was limited to the specific materials properties of both the concrete and the FRP composites. More studies have to be conducted with different material properties to give more proof and insights about the nature of the bond failure.

❖ The steel tensile stresses are with small values for the two layers of 2.4mm total thickness. These stresses occur at the location of debonding only with a big stress at the stirrups in which within debonding region. While, for other cases, more stresses are found in the flexural reinforcement only at the location of debonding.

❖ The interface bond-stresses are non-uniformly distributed along the reinforced boundaries. In particular, it is found that the shear stresses values exhibit peak values about 1 to 2 times greater than the mean values predicted by the classical beam theory.

❖ Therefore, the final recommendation drawn from this study is to use a wider layer of FRP composite rather than using two layers or even increasing the FRP thickness. Otherwise, it is better to use another strengthening configuration.

Data Availability Statement

All data, models, and code generated or used during the study appear in the submitted article.

References

[1] Khalifa, A. M. (2016). Flexural performance of RC beams strengthened with near surface mounted CFRP strips. Alexandria Engineering Journal, 55, pp. 1497-1505.

[2] Abdulrahman, B.Q. and Aziz, O.Q., 2021. Strengthening RC flat slab-column connections with FRP composites: A review and Comparative study. Journal of King Saud University-Engineering Sciences, 33, pp. 471-481.

[3] Ababneh, A.N., Al-Rousan, R.Z. and Ghaith, I.M., 2020, February. Experimental study on anchoring of FRP-strengthened concrete beams. In Structures (Vol. 23, pp. 26-33). Elsevier.

[4] Ascione, L. and Feo, L., 2000. Modeling of composite/concrete interface of RC beams strengthened with composite laminates. Composites Part B: Engineering, 31(6-7), pp.535-540.

[5] Yang, J., 2017. Interfacial Shear Stresses Calculation of FRP Strengthened RC Beams. Advances in Engineering Research, 6th International Conference on Energy, Environment and Sustainable Development.

[6] Ko, H., Matthys, S., Palmieri, A. and Sato, Y. (2014). Development of a simplified bond stress-slip model for bonded FRP–concrete interfaces. Construction and Building Materials, 68, pp. 142-157.

[7] López-González, J.C., Fernández-Gómez, J. and González-Valle, E., 2012. Effect of adhesive thickness and concrete strength on FRP-concrete bonds. Journal of Composites for Construction, 16(6), pp.705-711.

[8] Teng, J.G., Yuan, H. and Chen, J.F., 2006. FRP-to-concrete interfaces between two adjacent cracks: theoretical model for debonding failure. International journal of solids and structures, 43(18-19), pp.5750-5778.

[9] Wang, J., 2006. Cohesive zone model of intermediate crack-induced debonding of FRP-plated concrete beam. International journal of solids and structures, 43(21), pp.6630-6648.

[10] López, J., Fernández Gómez, J.A. and Gonzalez, E. Influencia de la relación tensión-deslizamiento en el comportamiento de la interfase FRP-hormigón. In: "IX Congreso Nacional de Materiales Compuestos, Girona, España. 2011:12799: pp.1-6. https://oa.upm.es/12799/

[11] Oehlers DJ, Moran JP. Premature failure of reinforced concrete beams. Struct Eng 1990;116:978–95.

[12] Granju JL. Debonding of thin cement-based overlays. Mater Civil Eng 2001;13:114–20.

[13] Sebastian WM. Significance of midspan debonding failure in FRP-plated concrete beams. Struct Eng 2001;127:792–8.

[14] Rabinovitch O, Frostig Y. Experiment and analytical comparison of RC beams strengthened with CFRP composites. Compos Part B 2003;34:663–77.

[15] Teng JG, Zhang JW, Smith ST. Interfacial stresses in reinforced concrete beams bonded with a soffit plate: a finite element study. Constr Build Mater 2002;16:1–14.

[16] Li, L.J., Guo, Y.C., Liu, F. and Bungey, J.H., 2006. An experimental and numerical study of the effect of thickness and length of CFRP on performance of repaired reinforced concrete beams. Construction and Building Materials, 20(10), pp.901-909.

[17] Harajli, M. H. and Soudki, K. A. (2003). Shear strengthening of interior slab-column connections using carbon fibre-reinforced polymer sheets. Journal of Composites for Construction, 7(2), pp.145-153.

[18] Garden, H.N., Hollaway, L.C. and Thorne, A.M. (1997). A preliminary evaluation of carbon fibre reinforced polymer plates for strengthening reinforced concrete members. Proceedings of the Institution of Civil Engineers. Structures and buildings, 122(2), pp.127-142.

[19] Buyle-Bodin, F., David, E. and Ragneau, E., 2002. Finite element modelling of flexural behaviour of externally bonded CFRP reinforced concrete structures. Engineering Structures, 24(11), pp.1423-1429.

[20] Chen, G. M., Teng, J. G., Chen, J. F. and Xiao, Q. G., (2015). Finite element modelling of debonding failures in FRP-strengthened RC beams: A dynamic approach. Computers and Structures, 158, pp.167-183.

[21] Leung, C.K., 2001. Delamination failure in concrete beams retrofitted with a bonded plate. Journal of Materials in Civil Engineering, 13(2), pp.106-113.

[22] Leung, C.K. and Tung, W.K., 2006. Three-parameter model for debonding of FRP plate from concrete substrate. Journal of Engineering Mechanics, 132(5), pp.509-518.

[23] Obaidat, Y. T., Heyden, S., Dahlblom, O., Abu-Farsakh, G. and Abdel-Jawad, Y. (2011). Retrofitting of reinforced concrete beams using composite laminates. Construction and Building Materials, 25(2), pp.591-597.

[24] Obaidat, Y. T., Heyden, S. and Dahlblom, O. (2010). The effect of CFRP and CFRP/concrete interface models when modelling retrofitted RC beams with FEM. Composite Structures, 92(6), pp.1391-1398.

[25] Grassl, P. and Jirásek, M. (2006). Damage-plastic model for concrete failure. International journal of solids and structures, 43(22), pp.7166-7196.

[26] Winkler, K. and Stangenberg, F. (2008). Numerical Analysis of Punching Shear Failure of Reinforced Concrete Slabs. ABAQUS User''s Conference, Newport, RI. Dassault Systemes, USA, Lowell, MA.

[27] British Standards Institution (BSI), (2004), Eurocode 2: Design of concrete structures – Part 1-1: General rules and rules for buildings.

[28] Nayal, R. and Rasheed, H. A. (2006). Tension stiffening model for concrete beams reinforced with steel and FRP bars. Journal of Materials in Civil Engineering, 18(6), pp. 831-841.

[29] Needleman, A., 1988. Material rate dependence and mesh sensitivity in localization problems. Computer methods in applied mechanics and engineering, 67(1), pp.69-85.

[30] Cornelissen, H. A. W., Hordijk, D. A. and Reinhardt, H. W. (1986). Experimental determination of crack softening characteristics of normal weight and lightweight concrete. Heron, 31(2), pp. 45-56.

[31] ACI Report 446.3R-97, (1997). Finite Element Analysis of Fracture in Concrete Structures: State-of-the-Art. Reported by ACI Committee 446.

[32] ABAQUS (2013). Theory Manual, User Manual and Example Manual, Version 6.12, Dassault Systemes Simulia Corp., Providence.

[33] Gay, D., Hoa, S. V. and Tsai, S. W. (2003). Composite materials design and applications. 1st ed. Boca Raton: CRC Press.

[34] Saleem, M.U., Khurram, N., Amin, M.N. and Khan, K., 2018. Finite element simulation of RC beams under flexure strengthened with different layouts of externally bonded fiber reinforced polymer (FRP) sheets. Revista de la Construcción. Journal of Construction, 17(3), pp.383-400.

[35] El-Sayed, W.E., Ebead, U.A. and Neale, K.W. (2005). Modelling of Debonding Failures in FRP-Strengthened Two-Way Slabs. Special Publication, 230, pp.461-480.

[36] Moslemi, M. and Khoshravan, M. (2015). Cohesive zone parameters selection for mode-I prediction of interfacial delamination. Strojniški vestnik-Journal of Mechanical Engineering, 61(9), pp.507-516.

[37] Lu, X. Z., Teng, J. G., Ye, L. P. and Jiang, J. J. (2005). Bond–slip models for FRP sheets/plates bonded to concrete. Engineering structures, 27(6), pp.920-937.

[38] Daud, R., Cunningham, L. and Wang, Y. (2015). Numerical study of effective bond length for externally bonded CFRP plate under cyclic loading. In A. J. Gill, and R. Sevilla (Eds.), Proceedings of the 23rd UK Conference of the Association for Computational Mechanics in Engineering. Swansea: University of Swansea, pp. 359-362.

[39] Daud, R., Cunningham, L. and Wang, Y. (2015). Non-linear FE Modelling of CFRP-strengthened RC slabs under cyclic loading, Athens Journal of Technology and Engineering, 2(3), pp.161-180.

[40] Abdulrahman, B.Q., Wu, Z. and Cunningham, L.S., 2017. Experimental and numerical investigation into strengthening flat slabs at corner columns with externally bonded CFRP. Construction and Building Materials, 139, pp.132-147.

[41] Savoia, M., Ferracuti, B. and Mazzotti, C., 2003. Non linear bond-slip law for FRP-concrete interface. In Fibre-Reinforced Polymer Reinforcement for Concrete Structures: (In 2 Volumes) (pp. 163-172).

[42] Chedad, A., Daouadji, T.H., Abderezak, R., Belkacem, A., Abbes, B., Rabia, B. and Abbes, F., 2017. A high-order closed-form solution for interfacial stresses in externally sandwich FGM plated RC beams. Advances in materials Research, 6(4), p.317.